Applied Mathematical Sciences, Vol. 8, 2014, no. 108, 5349 - 5359
HIKARI Ltd, www.m-hikari.com
http://dx.doi.org/10.12988/ams.2014.47580

Numerical Study of Staggered Scheme for Viscous Saint-Venant Equations

Putu Harry Gunawan[1,2]

[1]Institut Teknologi Bandung, Mathematics Department,
Jl. Ganesha No.10, Bandung, Indonesia, 40132
&
[2]Universitée Paris-Est & CNRS, LAMA UMR8050
F-77454, Marne-la-Vallée, France

Abstract

This paper describes a numerical scheme for approximate the viscous Saint-Venant equations. This scheme is called staggered grid scheme which is a robust, simple and strightforward scheme for viscous Saint-Venant equations. Some numerical simulations have been elaborated to validate the accuracy of the scheme, such as the calculation of the convergence rate L^1-norm error of the scheme, the comparison of viscous and classical Saint-Venant equations, comparison of staggered scheme with kinetic scheme and direct Navier-Stokes approach in dam-break problem and simulation of dry-wet problem. The results show good accuracy and in a good agreement with another scheme in another paper.

Mathematics Subject Classification: 35C20, 76B07, 76B25, 76M20

Keywords: Staggered grid, Saint-Venant equations, Viscosity, Dam-break

1 Introduction

The Saint-Venant equations (SVE) or known as shallow water equations are a set of hyperbolic partial differential equations which consist of two equations, mass conservation and momentum conservation. This equation is very

important to describe some fluid flow phenomenon such as, the water flow in channels or rivers, the sediment flow in estuaries, the gas flow in the atmosphere and etc (see [10]). The governing equations of one-dimensional classical SVE are written as

$$\partial_t h + \partial_x(hu) = 0, \tag{1}$$

$$\partial_t(hu) + \partial_x\left(hu^2 + \frac{1}{2}gh^2\right) + gh\partial_x z = 0, \tag{2}$$

where h is the total fluid depth, u is the velocity in the x direction, z is the topography, and g is the acceleration due to gravity. In these equations, the friction and viscosity term in momentum conservation are excluded. Moreover, the friction term is given based on the type of flow, for instance, in case of turbulent (Froude number $(Fr) > 1$), we often use Darcy-Weisbach's friction law. Whereas for the laminar $(Fr < 1)$ case, we often use Manning's friction law.

In this paper, we are interested to study the numerical scheme for viscous SVE in the laminar flow water model. This model was derived by Gerbeau and Perthame [3] which includes a friction, viscosity, and Coriolis-Boussinesq factor. The equations of one-dimensional viscous SVE are given as

$$\partial_t h + \partial_x(hu) = 0, \tag{3}$$

$$\partial_t(hu) + \partial_x\left(hu^2 + \frac{1}{2}gh^2\right) + gh\partial_x z = -\kappa_{\text{vsv}}(h)u + 4\mu\partial_x\left(h\partial_x u\right), \tag{4}$$

$$\kappa_{\text{vsv}}(h) = \frac{\kappa}{1 + \frac{\kappa h}{3\mu}}, \tag{5}$$

where h, u and z are the water height, the lateral velocity and the topography respectively. The gravitational force is define by g, and the constants κ and μ are the friction and viscosity coefficient respectively.

In order to approximate Eqs. (3 - 5), some methods have been proposed. For instance, in [3] they used the finite volume Kinetic scheme introduced by [1]. However, here we are interested using the finite volume staggered grid scheme for viscous SVE. This scheme is known as a robust and well-balanced scheme for classical SVE (1 - 2) (see [2, 5, 4] for the analysis of mathematical properties, i.e. consistency, stability, entropy satisfying, and see [2, 8, 9, 7] for the applications). Hence, in this paper we propose to construct and study the staggered scheme for viscous SVE.

The outline of this paper is given as, in Section 2, the numerical staggered scheme for viscous SVE is constructed. The numerical validation such as comparison of classical and viscous SVE in dam-break simulation and the convergence rate of L^1-norm error in various grid points are given in Section 3. Moreover, the comparison of staggered, kinetic and Navier-Stokes scheme

in laminar dam-break wet bed problem and also the study of dry-wet problem are examined. Finally in Section 4, the conclusions are organized.

2 Numerical scheme

Follow the notations of [2] and for the shake of simplicity, we consider the time interval $(0,T)$ is divided into N_t time steps of length Δt and, for all $n \in \{0,\dots,N_t\}$, $t^n := n\Delta t$. The domain $\Omega := (0,L)$ is divided into N_x cells of length Δx. The left end, the center and the right end of the i-th cell are denoted by $x_{i-\frac{1}{2}}$, x_i and $x_{i+\frac{1}{2}}$, respectively. We set $\mathcal{M} := \{1,\dots,N_x\}$, $\mathcal{E}_{int} := \{1,\dots,N_x-1\}$, $\mathcal{E}_b := \{0,N_x\}$, and $\mathcal{E} := \mathcal{E}_{int} \cup \mathcal{E}_b$.

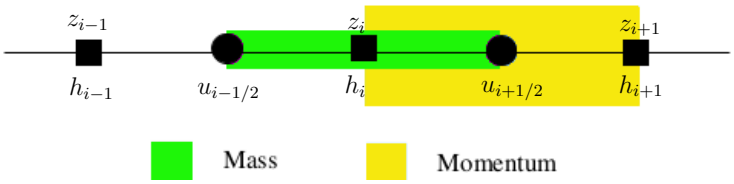

Figure 1: The one-dimensional space discretization staggered grids. The green area represents the control volume of mass for full points h_i and z_i. The control volume for conservation momentum for half point $u_{i+\frac{1}{2}}$ is shown by yellow area.

The water height h and the topography z are discretized at the center of the cells. The approximation of h and z at the point x_i and at time t^n is denoted by h_i^n and z_i^n respectively. The velocity u is discretized at the interfaces between the cells. The approximation of u at the point $x_{i+\frac{1}{2}}$ and at time t^n is denoted by $u_{i+\frac{1}{2}}^n$. This space discretization and the definition of control volume for mass and momentum are represented in Fig. 1.

The initial conditions are given as,

$$h_i^0 = \frac{1}{\Delta x}\int_{x_{i-\frac{1}{2}}}^{x_{i+\frac{1}{2}}} h_0(x)\,\mathrm{d}x, \qquad \forall i \in \mathcal{M}, \tag{6}$$

$$z_i^0 = \frac{1}{\Delta x}\int_{x_{i-\frac{1}{2}}}^{x_{i+\frac{1}{2}}} z_0(x)\,\mathrm{d}x, \qquad \forall i \in \mathcal{M}, \tag{7}$$

$$u_{i+\frac{1}{2}}^0 = \frac{1}{\Delta x}\int_{x_i}^{x_{i+1}} u_0(x)\,\mathrm{d}x, \qquad \forall i \in \mathcal{E}_{int}. \tag{8}$$

The discretization of mass conservation equation (3) is given as,

$$\frac{h_i^{n+1}-h_i^n}{\Delta t} + \frac{\left(F_{i+\frac{1}{2}}^n - F_{i-\frac{1}{2}}^n\right)}{\Delta x} = 0, \qquad \forall i \in \mathcal{M}. \tag{9}$$

where

$$F^n_{i+\frac{1}{2}} := \hat{h}^n_{i+\frac{1}{2}} u^n_{i+\frac{1}{2}}, \tag{10}$$

$$\hat{h}^n_{i+\frac{1}{2}} := \begin{cases} h^n_i & \text{if } u^n_{i+\frac{1}{2}} \geq 0 \\ h^n_{i+1} & \text{if } u^n_{i+\frac{1}{2}} < 0 \end{cases}, \qquad \forall i \in \mathcal{E}. \tag{11}$$

The momentum balance equation (4) is discretized with explicit upwind fluxes for the convection term, implicit centered fluxes for the pressure, semi-implicit for the friction term, and a second-order central difference for the viscosity term:

$$\frac{h^{n+1}_{i+\frac{1}{2}} u^{n+1}_{i+\frac{1}{2}} - h^n_{i+\frac{1}{2}} u^n_{i+\frac{1}{2}}}{\Delta t} + \frac{1}{\Delta x}\Big[F^n_{i+1}\hat{u}^n_{i+1} - F^n_i \hat{u}^n_i + \frac{1}{2}g\left((h^{n+1}_{i+1})^2 - (h^{n+1}_i)^2\right) + g h^{n+1}_{i+\frac{1}{2}}(z^0_{i+1} - z^0_i)\Big] + \kappa_{\text{vsv}}(h^{n+1}_{i+\frac{1}{2}})u^{n+1} - 4\mu\frac{1}{\Delta x}\Big[h^{n+1}_{i+1}\frac{(u^n_{i+\frac{3}{2}} - u^n_{i+\frac{1}{2}})}{\Delta x} - h^{n+1}_i \frac{(u^n_{i+\frac{1}{2}} - u^n_{i-\frac{1}{2}})}{\Delta x}\Big] = 0, \quad \forall i \in \mathcal{E}_{int}, \tag{12}$$

where

$$\kappa_{\text{vsv}}(h^{n+1}_{i+\frac{1}{2}}) := \frac{\kappa}{\left(1 + \dfrac{\kappa h^{n+1}_{i+\frac{1}{2}}}{3\mu}\right)}, \tag{13}$$

$$h^n_{i+\frac{1}{2}} := \frac{1}{2}\left(h^n_i + h^n_{i+1}\right), \qquad \forall i \in \mathcal{E}_{int}, \tag{14}$$

$$F^n_i := \frac{1}{2}\left(F^n_{i-\frac{1}{2}} + F^n_{i+\frac{1}{2}}\right), \tag{15}$$

$$\hat{u}^n_i := \begin{cases} u^n_{i-\frac{1}{2}} & \text{if } F^n_i \geq 0 \\ u^n_{i+\frac{1}{2}} & \text{if } F^n_i < 0 \end{cases}, \qquad \forall i \in \mathcal{M}. \tag{16}$$

The topography is not evolving in time, therefore in (12) the discretization of topography remains using the initial condition. In order to keep the stability of the scheme (i.e the water height remains non-negative at time t^{n+1}), the Courant-Friedrichs-Lewy (CFL) condition is given by

$$\Delta t := \frac{\nu \Delta x}{\max\limits_{i \in \mathcal{M}} \left(\dfrac{\left|F^n_{i+\frac{1}{2}} + F^n_{i-\frac{1}{2}}\right|}{2h^n_i} + \sqrt{g h^n_i}\right)}, \tag{17}$$

where the Courant number is given by $\nu \leq 1$. Note that in the previous scheme (9)-(16), we only consider the first order of accuracy in space and time.

Remark 2.1 (Second order scheme)**.** *Second-order accuracy in space and time can be achieved with usual technique for example, MUSCL or ENO flux reconstruction for the space, and Heun method for the time.*

Important to note that, in order to avoid the presence of non-entropic shock in our numerical simulation, we used $\frac{1}{2}g\left[(h_{i+1}^{n+1})^2 \text{ - } (h_i^{n+1})^2\right]$ instead of $\frac{1}{2}g\left[(h_{i+1}^{n})^2 \text{ - } (h_i^{n})^2\right]$ in momentum conservation (see [2] for more detail). Finally, the general algorithm is given in Algorithm 1.

Algorithm 1 The explicit staggered scheme.

Step 1. Give the initial conditions at $n = 0$.

Step 2. Compute (10 - 11) for $F^n_{i+\frac{1}{2}} \forall i \in \mathcal{E}_{int}$.

Step 3. Compute (17) for Δt to preserve the stability.

Step 4. Solve (9) for $h_i^{n+1} \quad \forall i \in \mathcal{M}$.

Step 5. Solve (12) for $h^{n+1}_{i+\frac{1}{2}} u^{n+1}_{i+\frac{1}{2}} \quad \forall i \in \mathcal{E}_{int}$ and immediately we can get $u^{n+1}_{i+\frac{1}{2}}$.

3 Numerical tests

In this section, we elaborate two numerical tests such as dam-break on a wet and dry bed simulations.

3.1 Dam-break on a wet bed

In this simulation, first we will examine the comparison between classical and viscous SVE. Here the domain is $\Omega = [-50 : 50]$ ($L = 100$ m length) and the initial conditions are given as

$$h_{\text{ini}}(x) = \begin{cases} h_l & \text{if } x \leq 0 \\ h_r & \text{otherwise} \end{cases}, \tag{18}$$

$$z_{\text{ini}}(x) = 0, \tag{19}$$

$$u_{\text{ini}}(x) = 0, \tag{20}$$

where $h_l = 2$, $h_r = 1$, the boundary conditions are set to be wall in the both boundaries and the CFL condition is set to be 1. For the viscous SVE, the coefficients of friction and viscosity term are given as $\kappa = 0$ and $\mu = \dfrac{h_l - h_r}{L}$ respectively.

In Fig. 2, the results of water level and velocity are shown at final time $t = 7$ s. Fig. 2(b) and 2(c) show the zoom part of Fig. 2(a) in rarefaction (A1) and shock (A2) waves of water level respectively. We can see clearly that, in

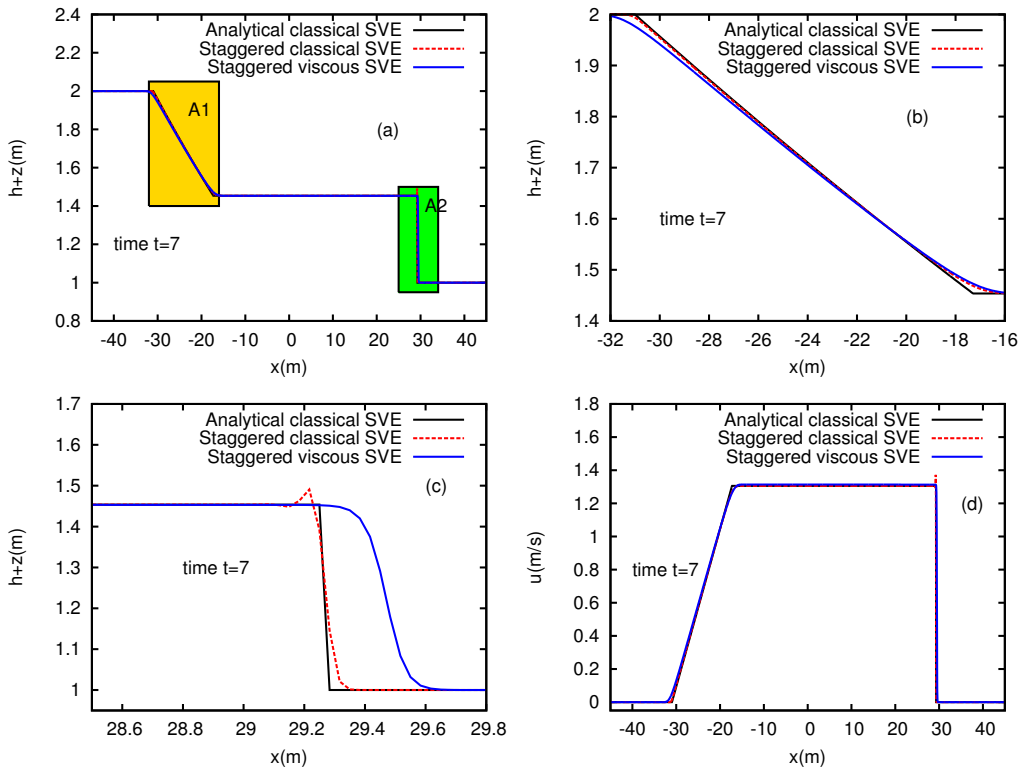

Figure 2: Dam-break on a wet bed. (a) The comparison of water level profile on full domain.(b) The zoom area of (A1) on the rarefaction wave. (c) The zoom area of (A2) on the shock wave. (d) The velocity profile on full domain. The CFL condion is 1 and final time $t = 7$ s.

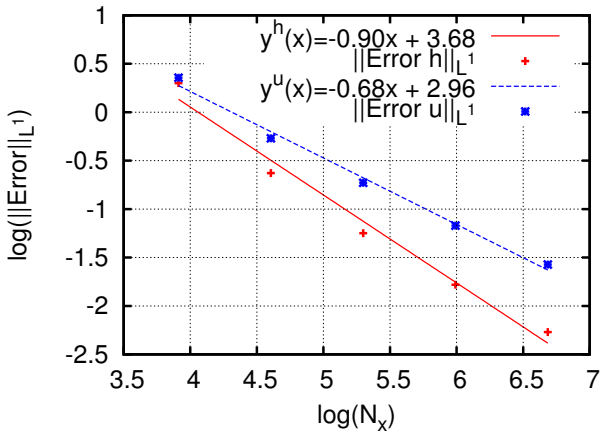

Figure 3: The convergence rate of L^1-norm error of h and u in various grid points N_x. The functions $y^h(x)$ and $y^u(x)$ are obtained from data fitting of L^1-norm error of h and u respectively using the nonlinear least-squares method.

the shock area, the numerical result in viscous SVE is more diffusive thus the oscillation in shock area vanished. Contrary, the staggered scheme for classical SVE in dam-break simulation produces small bump in the shock area (which is not due to numerical instability), however it is more accurate than the other robust methods (see [2] for more illustrations and explanations). Moreover, we can confirm that the shock speed in viscous SVE is faster than the classical SVE. On the other hand, in rarefaction wave and intermediate depth are quite similar in both cases.

In this test case, there is no analytical solution for dam-break in viscous SVE. Therefore, in order to evaluate the accuracy of the scheme, we used a reference solution. Here, a reference solution is computed by using a very fine mesh of 3200 grid points. Hence the L^1-norm error is calculated by $||\text{Error } \Phi||_{L^1} = \int_\Omega |\Phi(x) - \Phi_{\text{ref}}(x)| \, \mathrm{d}x$, where Φ could be either h or u. The convergence rate of L^1-norm error both in h and u, in various grid points N_x are shown in Fig. 3. We can observe that, in Fig. 3 the convergence of our scheme ameliorates along with the increasing of numbers of grid points as we expected.

Next, it will be interesting if we elaborate our scheme into a numerical simulation of viscous dam-break introduced in [6, 3]. Here, we will compare the results of our scheme with the results of Kinetic scheme (see [1]) and direct Navier-stokes obtained in [3]. In this simulation, the domain and the initial conditions are given as in the previous simulation. However, in order to get the same simulation in [3], the gravitational force and two final time steps are modified as $g = 2$ m/s^2, $t = 5$ s and $t = 10$ s.

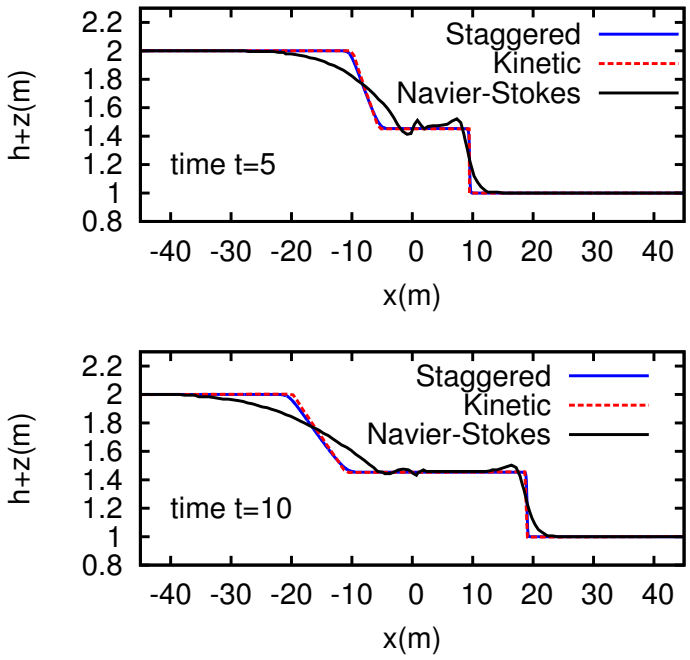

Figure 4: Dam-break viscous SVE. The series of water level $h + z$ profiles at final times $t = 5$ s and $t = 10$ s.

The results of these simulation are shown in Fig. 4. They show that our scheme is comparable with the Kinetic scheme for viscous SVE. In addition, comparing with the result using direct Navier-Stokes in Fig. 4, all schemes have a same shock speed and intermediate water depth. The comparison of the intermediate water depth in various values of κ is shown in Fig. 5. They show that the given of various κ produce difference profiles.

3.2 Dam-break on a dry bed

The aim of this simulation is not only to examine the ability of the scheme to handle vacuum, but also to confirm the ability to deduct non-smooth topography. Here the domain is $\Omega = [-50 : 50]$ m and the initial conditions are given as

$$z_{\text{ini}}(x) = \begin{cases} 1 & \text{if } -30 < x < -20 \\ 0.2(x-20) & \text{if } x > 20 \\ 0. & \text{otherwise} \end{cases}, \tag{21}$$

$$(h+z)_{\text{ini}}(x) = \begin{cases} \max(2, z_{\text{ini}}(x)) & \text{if } x \le 0 \\ \max(1, z_{\text{ini}}(x)) & \text{otherwise} \end{cases}, \tag{22}$$

$$u_{\text{ini}}(x) = 0. \tag{23}$$

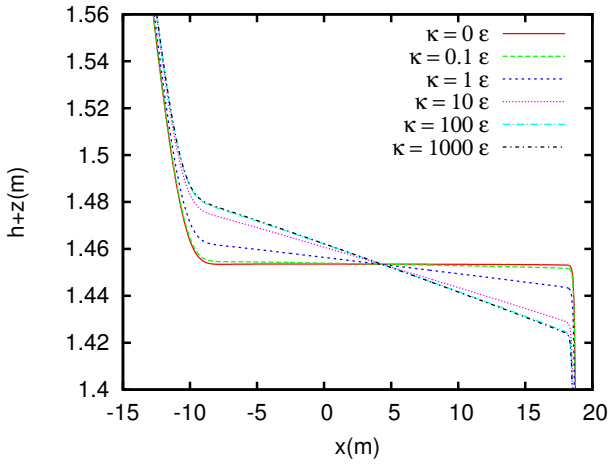

Figure 5: Dam-break on a wet bed of viscous SVE. The comparison of the intermediate water level $h + z$ profiles with various κ where $\epsilon = \frac{h_l - h_r}{L}$.

The boundary conditions are set to be zero at the end of left and right domain. The CFL condition is used is 1 and the coefficients of friction and viscosity are given as $\kappa = 10\epsilon$ and $\mu = \epsilon$ respectively with $\epsilon = \frac{h_l - h_r}{L}$. Results from various final time steps ($t = 0$, $t = 13$, $t = 20$ and $t = 30$) are shown in Fig. 6. Here, we can see clearly that the scheme is perfectly able to treat dry-wet transitions and also to handle the non-smooth topography. Moreover, we also can confirm that our scheme produces the waves over the jumps of topography.

4 Conclusion

The staggered grid scheme for viscous Saint-Venant equations has been presented. This scheme is simple, accurate and strightforward both for viscous and classical Saint-Venant equations. The good convergence rate of L^1-norm error in h and u are shown nicely increasing along with the increasing number of points. Some comparison results from other schemes are elaborated in dam-break problem. They have a good agreement with the another results using Kinetic scheme and direct Navier-Stokes approach. Moreover, through the simulation of dam-break on a dry bed, we can confirm that our scheme is able to handle vacuum and non-smooth topography. Finally, we can conclude that staggered grid scheme is a robust scheme for viscous SVE.

Acknowledgements. The author would like to thank to DIKTI and Riset Desentralisasi 1063c/I1.C01.2/PL/2014 for the financial support, to Ms. S.R.Pudjaprasetya (Mathematics, ITB) and Mr. Christian Naa (Physics, ITB,

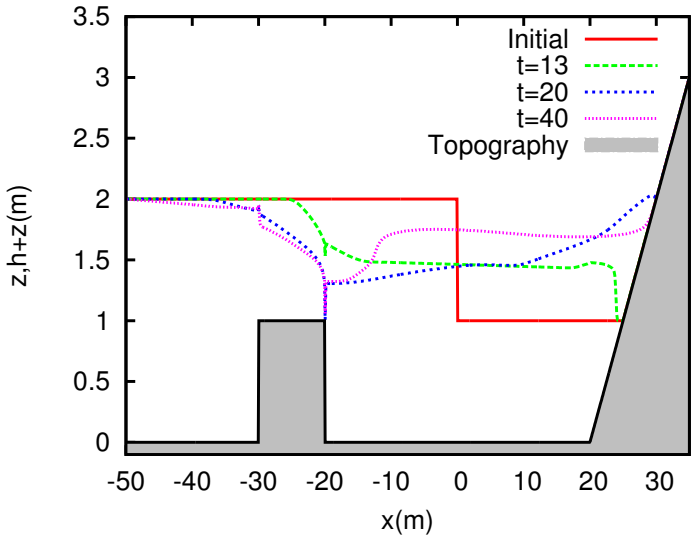

Figure 6: Dam-break on a dry bed of viscous SVE. The comparison of water level $h + z$ profiles with various final time steps.

ULCO) for the motivation.

References

[1] E. Audusse, M.-O. Bristeau, and B. Perthame. Kinetic Schemes for Saint-Venant Equations with Source Terms on Unstructured Grids. Rapport de recherche RR-3989, INRIA, 2000. Projet M3N.

[2] D. Doyen and P. H. Gunawan. An explicit staggered finite volume scheme for the shallow water equations. In *Finite Volumes for Complex Applications VII-Methods and Theoretical Aspects*, pages 227–235. Springer, 2014.

[3] J.-F. Gerbeau, B. Perthame, et al. Derivation of viscous saint-venant system for laminar shallow water; numerical validation. 2000.

[4] R. Herbin, J.-C. Latché, and T. T. Nguyen. Explicit staggered schemes for the compressible euler equations. In *ESAIM: Proceedings*, volume 40, pages 83–102. EDP Sciences, 2013.

[5] R. Herbin, n. W.Kheriji, and n. J.C.Latch. On some implicit and semi-implicit staggered schemes for the shallow water and euler equations. *ESAIM: Mathematical Modelling and Numerical Analysis*, eFirst:1290–3841, 4 2014.

[6] A. Huerta and W. K. Liu. Viscous flow with large free surface motion. *Computer Methods in Applied Mechanics and Engineering*, 69(3):277–324, 1988.

[7] S. R. Pudjaprasetya and I. Magdalena. Momentum conservative scheme for shallow water flows. *East Asian Journal on Applied Mathematics (EAJAM)*, 4(2):152–165, 2014.

[8] G. Stelling and S. Duinmeijer. A staggered conservative scheme for every froude number in rapidly varied shallow water flows. *International Journal for Numerical Methods in Fluids*, 43(12):1329–1354, 2003.

[9] G. Stelling and M. Zijlema. An accurate and efficient finite-difference algorithm for non-hydrostatic free-surface flow with application to wave propagation. *International Journal for Numerical Methods in Fluids*, 43(1):1–23, 2003.

[10] C. B. Vreugdenhil. *Numerical methods for shallow-water flow*, volume 13. Springer, 1994.

Received: July 9, 2014